

Article

Electric Vehicle Charging Load Demand Forecasting in Different Functional Areas of Cities with Weighted Measurement Fusion UKF Algorithm

Minan Tang ^{1,*}, Xi Guo ¹, Jiandong Qiu ², Jinping Li ¹ and Bo An ³

¹ College of New Energy and Power Engineering, Lanzhou Jiaotong University, Lanzhou 730070, China; 11220941@stu.lzjtu.edu.cn (X.G.); 11220936@stu.lzjtu.edu.cn (J.L.)

² College of Electrical and Mechanical Engineering, Lanzhou Jiaotong University, Lanzhou 730070, China; qjuid@mail.lzjtu.cn

³ College of Automation and Electrical Engineering, Lanzhou Jiaotong University, Lanzhou 730070, China; 12211434@stu.lzjtu.edu.cn

* Correspondence: tangminan@mail.lzjtu.cn

Abstract: The forecasting of charging demand for electric vehicles (EVs) plays a vital role in maintaining grid stability and optimizing energy distribution. Therefore, an innovative method for the prediction of EV charging load demand is proposed in this study to address the downside of the existing techniques in capturing the spatial–temporal heterogeneity of electric vehicle (EV) charging loads and predicting the charging demand of electric vehicles. Additionally, an innovative method of electric vehicle charging load demand forecasting is proposed, which is based on the weighted measurement fusion unscented Kalman filter (UKF) algorithm, to improve the accuracy and efficiency of forecasting. First, the data collected from OpenStreetMap and Amap are used to analyze the distribution of urban point-of-interest (POI), to accurately classify the functional areas of the city, and to determine the distribution of the urban road network, laying a foundation for modeling. Second, the travel chain theory was applied to thoroughly analyze the travel characteristics of EV users. The Improved Floyd (IFloyd) algorithm is used to determine the optimal route. Also, a Monte Carlo simulation is performed to estimate the charging load for electric vehicle users in a specific region. Then, a weighted measurement fusion UKF (WMF–UKF) state estimator is introduced to enhance the accuracy of prediction, which effectively integrates multi-source data and enables a more detailed prediction of the spatial–temporal distribution of load demand. Finally, the proposed method is validated comparatively against traffic survey data and the existing methods by conducting a simulation experiment in an urban area. The results show that the method proposed in this paper is applicable to predict the peak hours more accurately compared to the reference method, with the accuracy of first peak prediction improved by 53.53% and that of second peak prediction improved by 23.23%. The results not only demonstrate the high performance of the WMF–UKF prediction model in forecasting peak periods but also underscore its potential in supporting grid operations and management, which provides a new solution to improving the accuracy of EV load demand forecasting.



Citation: Tang, M.; Guo, X.; Qiu, J.; Li, J.; An, B. Electric Vehicle Charging Load Demand Forecasting in Different Functional Areas of Cities with Weighted Measurement Fusion UKF Algorithm. *Energies* **2024**, *17*, 4505. <https://doi.org/10.3390/en17174505>

Academic Editor: Rajendra Singh Adhikari

Received: 27 July 2024

Revised: 5 September 2024

Accepted: 5 September 2024

Published: 8 September 2024



Copyright: © 2024 by the authors. Licensee MDPI, Basel, Switzerland. This article is an open access article distributed under the terms and conditions of the Creative Commons Attribution (CC BY) license (<https://creativecommons.org/licenses/by/4.0/>).

1. Introduction

The popularization of electric vehicles provides an effective solution to achieving the dual-carbon goal, preventing air pollution more effectively, promoting energy transformation, and diversifying the mode of transportation. In recent years, the ownership of electric vehicles has been increasing annually due to both government incentives and marketing. As electric vehicle charging load demand shows uncertainty in time and space, the accurate and efficient prediction of charging demand is conducive to ensuring the stability of power

system operation. Moreover, it can improve the utilization rate of charging facilities, which is essential for charging facility site selection and urban planning. At present, plenty of studies have been conducted on forecasting the load of electric vehicles, with a series of research results obtained. In practice, the charging load is affected by various factors, and there is a certain degree of randomness in its spatial and temporal distribution. Consequently, it is difficult to predict the load. Typically, the construction of a load prediction model requires that consideration be given to various factors, including the size of electric vehicles, charging mode, operational patterns, battery characteristics, and tariff systems. Hua and Wang proposed an orderly charging load forecasting method for electric vehicles traveling in residential areas based on electric vehicle ownership and charging probability prediction. However, the electric load characteristics of electric vehicle users in urban residential areas are not applicable to the practice of electric vehicle load demand forecasting in other functional areas [1]. Luo and Hu analyzed the charging law that applies to different types of electric vehicles, with a Monte Carlo simulation performed to determine the charging load demand of various electric vehicles in the city. However, the traffic network model was not constructed, and the impact of traffic flow changes on the driving time and path of electric vehicles was ignored. As a result, it was difficult to predict the spatial distribution characteristics of charging load more effectively [2]. Through the probabilistic fitting of EV users' travel patterns, Yi and Li established a charging probability model that takes into account travel uncertainty and calculated EV charging load curves. However, there are some variations in the pattern of travel between different types of electric vehicles, which are overlooked in the article [3]. Chen put forward a method of predicting the spatial and temporal distribution of electric vehicle charging loads according to dynamic traffic information, with consideration given to the impact of traffic and road network information on electric vehicle driving patterns. However, there was no analysis of the differences in the charging load demand of electric vehicle users in different functional areas of the city [4]. Shafqat presented an EV spatial-temporal approach to load mobility forecasting for the robust estimate of charging load mobility [5]. Ding established a semi-dynamic traffic network model by considering the division of urban functional areas. By simulating the travel behavior of private cars and cabs with the improved travel chain and OD matrix, a charging load prediction method was proposed for private cars and cabs under the guidance strategy. With external factors taken into account, it provides a reference for the spatial-temporal distribution of the load of electric vehicles in the city [6]. Zhang proposed a method that can be used to predict electric vehicle charging demand based on urban grid attribute division. By considering the charging behavior characteristics of electric vehicles, a complete charging demand prediction model was established for different functional areas in the city. However, it is necessary to improve the accuracy of load demand forecasting [7]. Aduama and Zhang developed a prediction method based on multi-feature data fusion, with consideration given to weather conditions to improve the accuracy of the deep-learning model used for electric vehicle charging load forecasting. However, there are variations by region in the applicability of the analysis of environmental conditions varies [8]. The Monte Carlo algorithm is applied more to electric vehicle load demand forecasting. In recent years, many studies have been carried out to develop various forecasting optimization algorithms, for improving the accuracy of electric vehicle load demand forecasting. Xu and Chen adopted the forecasting model incorporating multiple forecasting models to predict conventional vehicle ownership, proposing an improved BUSS model based on the number of electric vehicles and presenting a Monte Carlo simulation-based electric vehicle conformity demand forecasting model. This contributes novel ideas to load demand modeling [9]. Yang proposed a method of federated learning electric vehicle short-term charging load prediction by taking into account user charging behavior and privacy protection [10]. By integrating the travel influencing factors of electric vehicle users, Chen simulated the travel habits of electric private cars, electric buses, and electric cabs in the city with the Monte Carlo method used to predict the charging load demand of electric vehicles in the city. However, this method is relatively homogeneous and ineffective in improving

the accuracy of prediction [11]. Zhang and Wang considered the effects of real-time traffic and temperature to propose a spatial-temporal distribution prediction method for urban electric vehicle charging loads, which is based on stochastic path simulation of the Markov decision-making process. However, the accuracy of charging load demand forecasting is unsatisfactory [12], although the stochastic nature of electric vehicle driving paths is carefully considered. Zhou presented an improved robust over-time optimization method using the scenario method for renewable energy sources with uncertainty to minimize the daily operating cost of the power system [13]. Li put forward an electric vehicle charging load prediction method based on ArcGIS road network structure and traffic congestion analysis [14]. Zhang and Tao adopted the Monte Carlo method to model the charging behavior of EV users, proposing a dynamic weight distribution method that combines the prediction results of two methods, namely deep confidence network and long and short-term memory network. Thus, the accuracy of load prediction can be improved. This new method provides a different perspective on eliminating the uncertainties in the prediction process [15]. Zhou integrated Long Short-Term Memory (LSTM) networks with Bayesian probabilistic theory to capture the uncertainty in forecasting for the improved accuracy of load forecasting [16]. Liu proposed an improved Kalman filter algorithm to forecast the short-term load of electric power, which leads to a higher accuracy of forecasting. This improved algorithm contributes a novel solution to short-term load forecasting [17]. Li and Sun presented a nonlinear weighted measurement fusion unscented Kalman filter, demonstrating its applicability to reduce target uncertainty, improve tracking accuracy, and lower computationally burdensome compared to centralized fusion unscented Kalman filter algorithms. Also, it can be used for the nonlinear prediction of electric vehicle load demand [18].

Table 1 lists a summary of the above literature on EV charging load forecasting by the year of publication, in ascending order.

Table 1. Literature review of EV charging load prediction.

Reference Number	Model/Technique	Location	Performance	Limitation
[19]	Deep-learning and Spatial-Temporal analysis	China	Improved forecasting accuracy	High data requirements and long training times
[20]	Machine learning model	Multiple countries around the world	Broad coverage and comprehensive approach	Lack of scenario-specific in-depth analysis
[21]	Conditional variational auto-encoder	China	For complex charging demand forecasts	Complex models with high computational resource requirements
[22]	Machine learning and Spatial-Temporal analysis	USA	Joint consideration of space and time factors works well	Dependent on high quality datasets
[23]	Comparison of multiple deep-learning techniques	European	Optimize the performance of different models to provide instructive results	Insufficient detailed analysis of specific algorithms

Despite the existing studies that have contributed significantly to EV load demand forecasting and taken into account the uncertainties in this process, there remains room for improvement in the accuracy of forecasting, particularly the temporal and spatial distribution of load demand. To address this issue, an innovative forecasting method is presented in this paper to predict the spatial and temporal distribution of EV load demand in an optimal way. This method takes into account a wide range of factors, including the division of urban functional zones, the travel characteristics of EV users, and the accuracy of charging load demand prediction. By applying the weighted measurement fusion unscented Kalman filter (WMF–UKF) algorithm, a cutting-edge nonlinear filtering technique was developed to approximate the Gaussian distribution of a nonlinear function through the sigma points, which addresses the complexity in the computation of Jacobian matrices in the conventional extended Kalman filter (EKF). The weighted measurement fusion method enables a thorough statistical analysis of multi-source and multi-temporal sensor data, effectively integrating multi-dimensional information through the assignment of appropriate weights to different data based on mathematical methods and practical experience. With the introduction of the incremental observation equation, the prediction error associated with the unknown quantity of the system can be eliminated to enhance the accuracy of state estimation for the under-observed system. Not limited to the short-term forecasting of load demand, this study focuses on elucidating the characteristics of spatial and temporal distributions, which provides more accurate decision-making support for maintaining the stability of the power grid and optimizing the configuration of charging facilities.

This paper aims to address the severe delays, uncertainties, and nonlinearity in urban EV charging. This is because these problems disrupt the forecasting of EV charging load demand, especially in the case of uneven spatial and temporal distribution and low accuracy of forecasting. Therefore, a novel approach to urban electric vehicle load demand forecasting is put forward in this paper, with innovation achieved in the following aspects. (1) Functional zoning: The city was divided into functional zones for accurately forecasting the distribution of EV load demand across different functional zones. This approach contributes to revealing the differences in load demand within cities, which enables more targeted forecasts. (2) Road network topology model: An urban road network topology model was constructed to comprehensively evaluate the impact of traffic flow on travel path selection and the travel time of EV users. (3) Weighted measurement fusion combined with UKF: The combination of weighted measurement fusion with the unscented Kalman filter (UKF) algorithm effectively eliminates the impact of unknown measurement errors in the system, therefore significantly enhancing the accuracy of forecasting. This innovative approach is of great significance in addressing uncertainty and nonlinearity. (4) Method validation: The high accuracy of the weighted measurement fusion UKF algorithm in load demand forecasting was verified by comparatively analyzing the method with the actual traffic network data and other methods as a reference. This empirical analysis illustrates the effectiveness of this method, providing a reference for future research. In summary, a systematic approach to forecasting the load demand for urban electric vehicle charging is proposed in this paper.

The remainder of this paper is set out as follows. The travel pattern of users is analyzed in Section 3. The load demand forecasting model for electric vehicles is developed in Section 4. The effectiveness of the proposed strategy is verified in Section 5. Finally, conclusions are given in Section 6. The structure of the article is shown in Figure 1.

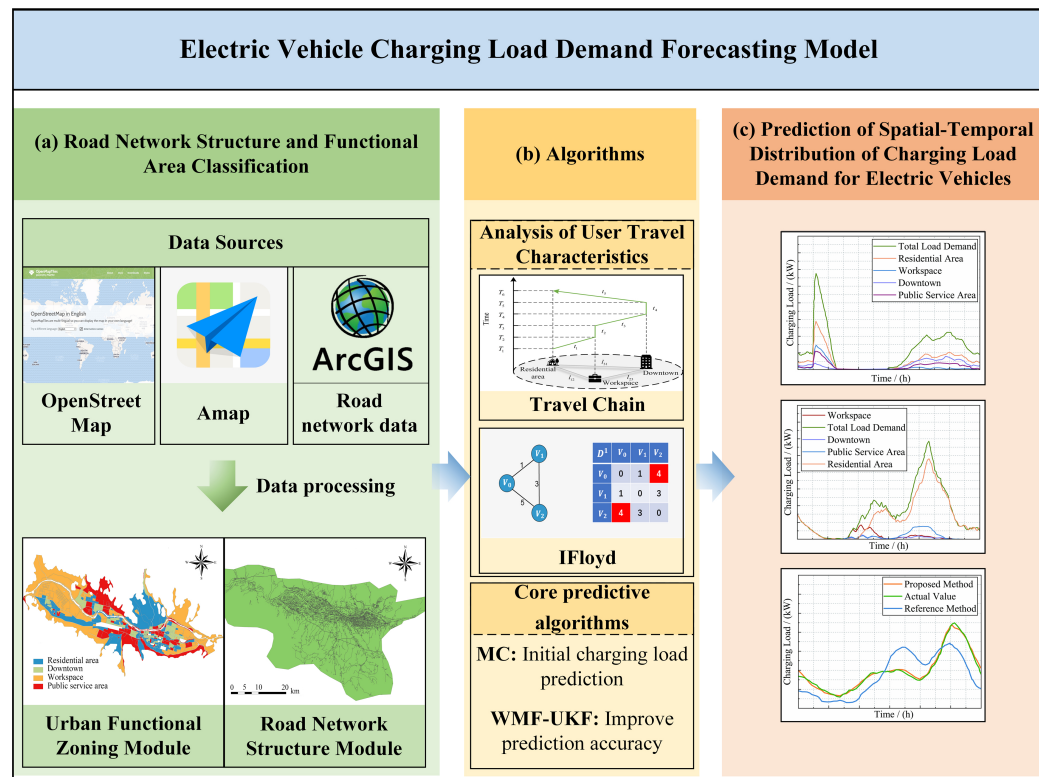


Figure 1. Structural diagram.

2. Urban Functional Zoning Divide and Road Network Modeling

2.1. Urban Functional Zoning Divide

This paper analyses the demand for electric vehicle charging in different functional areas of a region. It obtains POI values for each area from Amap for reclassification and combines OpenStreetMap, nighttime lighting, and Tencent social big data as input features. The area is categorized into four major functional zones based on the functions of urban plots: residential area, downtown, workspace, and public service area [19], as shown in Figure 2.

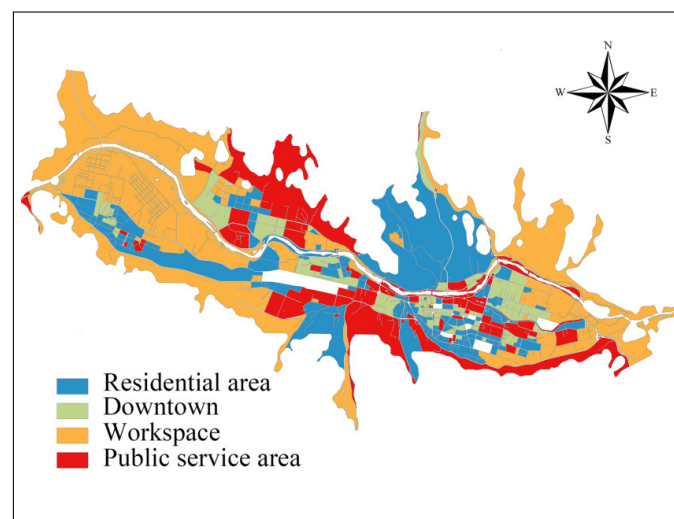


Figure 2. Functional area classification map of Anning District, Lanzhou city.

2.2. Urban Road Network Modeling

This paper analyses road data in the study area obtained from the OpenStreetMap open-source map data community and imported into ArcGIS. The required data, such as

highways, major roads, and minor roads, were retained based on their data attributes, while irrelevant road sections, such as footpaths, bicycle paths, and parkways, were excluded [20]. The processed road network data consists of 17,036 lines of data, and the road network structure is shown in Figure 3.

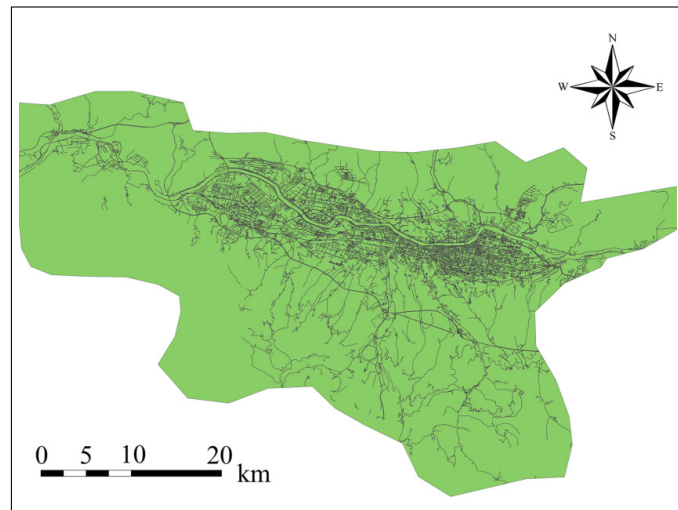


Figure 3. Structure of the road network in Anning district, Lanzhou City.

The road topology in one of the regions where the road network structure is modeled is shown in Figure 4. All road segments are assumed to be bi-directional, and the matrix D represents the adjacency matrix of road segment lengths and node connections. The matrix D is shown in Equation (1).

$$D = \begin{bmatrix} 0 & l_{12} & l_{13} & \infty & \infty \\ l_{21} & 0 & \infty & l_{24} & l_{25} \\ l_{31} & \infty & 0 & l_{34} & l_{35} \\ \infty & l_{42} & l_{43} & 0 & l_{45} \\ \infty & l_{52} & l_{53} & l_{54} & 0 \end{bmatrix} \quad (1)$$

where l_{ij} is the length of the road section between road nodes i and j , which can be obtained from the length l attribute in the road class attribute table in ArcGIS, $i, j \in n, n$ is the total number of road nodes; ∞ indicates that the distance between the two road nodes is infinite, i.e., the two nodes are not connected; according to the matrix D , the shortest path can be obtained from the shortest path algorithm for each node.

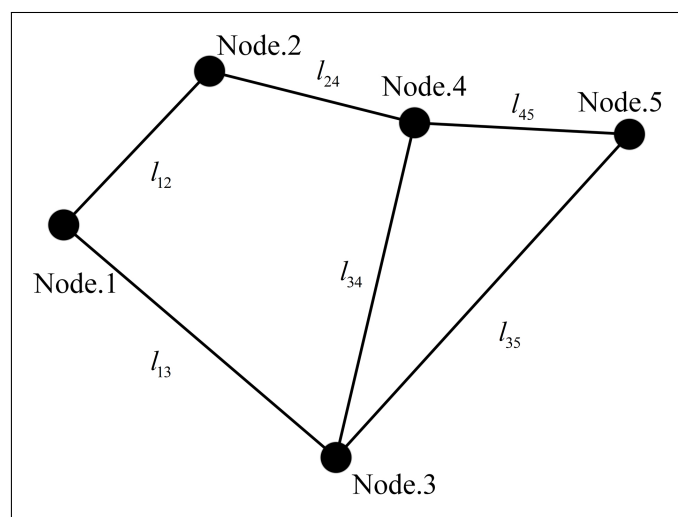


Figure 4. Road topology map.

3. Characterization of Travel Profiles of Electric Vehicle Users

3.1. Travel Patterns of Electric Vehicle Users

The charging time for electric vehicle users is influenced by several factors, including the type of vehicle, individual travel habits, battery capacity, and seasonal and holiday variations [21]. This paper focuses on the daily travel demand for electric private cars and electric taxis in urban areas. The data used are taken from the National Bureau of Statistics, and the initial charging time and the daily mileage of electric vehicles follow a normal distribution [22].

Figure 5 illustrates that the initial charging time for electric vehicles can be divided into two periods: 0–12 h and 12–24 h. The probability density function follows a normal distribution as Equation (2) shows [23]. The fitting parameters for initial charging time are shown in Table 2.

$$T_S = \begin{cases} \frac{1}{\sigma_t \sqrt{2\pi}} \exp\left(-\frac{(t + 24 - \mu_t)^2}{2\sigma_t^2}\right), & 0 \leq t \leq \mu_t - 12 \\ \frac{1}{\sigma_t \sqrt{2\pi}} \exp\left(-\frac{(t - \mu_t)^2}{2\sigma_t^2}\right), & \mu_t - 12 \leq t \leq 24 \end{cases} \quad (2)$$

where μ_t is the mean of initial charging time; σ_t is the variance of initial charging time. The specific fitting parameters are shown in Table 1.

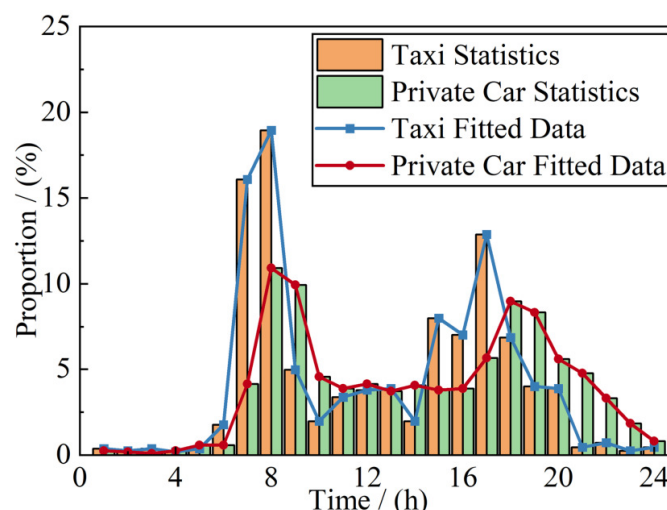


Figure 5. Distribution of initial charging time for electric vehicles.

Table 2. Fitting parameters for initial charging time.

Vehicle Type	Private Car		Taxi	
Time/(h)	0–12	12–24	0–12	12–24
Expectation/(min)	488.6	1055.5	450.1	1085.5
Variance/(min ²)	122.1	167.1	82.7	135.7

The state of charge of an electric vehicle's battery has a direct impact on the user's charging behavior. The probability of an electric vehicle user choosing to charge or not is related to their charging habits and level of anxiety about mileage. The analysis of charging behavior in a city has led to the derivation of the probability distribution of the starting state of charge for electric vehicles [24], as shown in Figure 6.

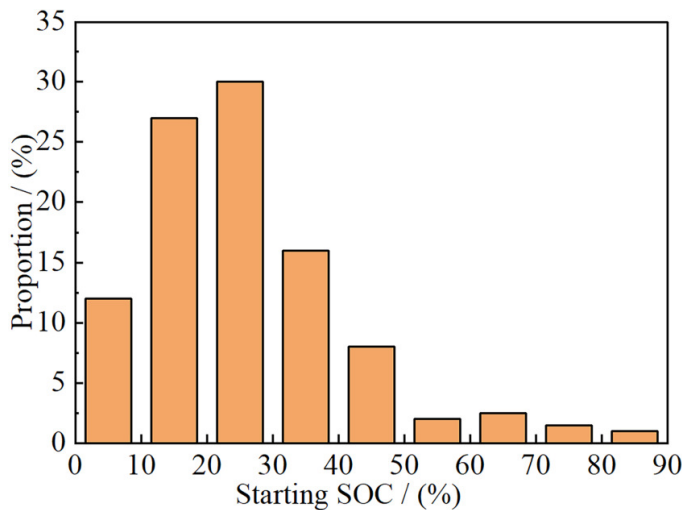


Figure 6. Derivation of the probability distribution of the starting SOC.

The mileage of private cars is influenced by various factors. Private cars are primarily used for work and recreation. As depicted in Figure 7, there is a significant difference in mileage between weekdays and rest days. The daily mileage of electric vehicles was fitted using SPSS 26 software [25]. The probability distribution of trips by private car is shown in Equation (3).

$$g(l) = \frac{1}{D\sigma_l \sqrt{2\pi}} \exp\left(-\frac{(\ln l - \mu_l)^2}{2\sigma_l^2}\right), l > 0 \quad (3)$$

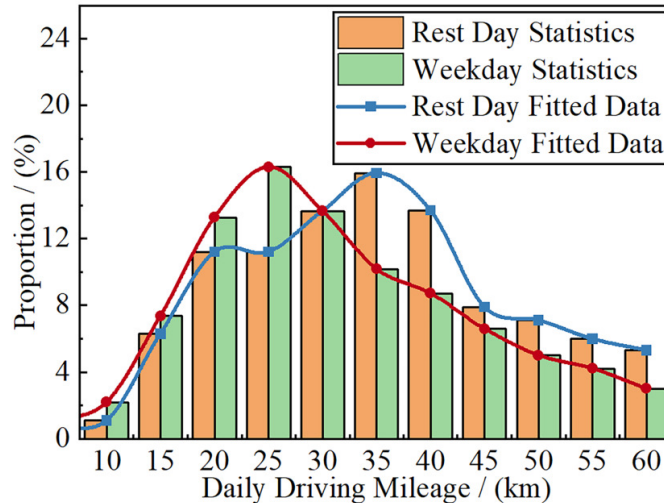


Figure 7. Distribution of daily driving mileage for private electric cars.

The daily mileage of taxis is a complex matter, influenced by factors such as the frequency of choice of taxi drivers and city demand. On average, the mileage ranges between 300 and 600 km and follows a normal distribution. The fitted parameters for daily driving mileage are shown in Table 3.

Table 3. Fitting parameters for daily driving mileage.

Vehicle Type	Taxi
Time/(h)	0–12
Expectation/(km)	335.7
Variance/(km ²)	224.5
	12–24
	265.4
	225.4

The duration of electric vehicle charging is primarily influenced by the SOC, battery charging power, and battery capacity. Therefore, the charging duration is shown in Equation (4) [25].

$$T_c = \frac{(1 - SOC_k)Q}{P} \quad (4)$$

3.2. Travel Characteristics of Users Based on Travel Chain Theory

The spatial-temporal distribution of electric vehicle users' charging load is closely related to their traveling patterns. Therefore, when analyzing users' traveling characteristics, it is important to consider their spatial-temporal characteristics. This paper presents the travel chain model, which simulates the travel characteristics of users in a day [26]. Private car owners have two types of travel chains: simple and complex. The simple chain is a closed-loop structure that includes only one travel destination, while the complex chain includes multiple travel destinations, passing through residential areas, workspaces, and downtown, which are the target endpoints, and ultimately returning to the starting point.

This paper analyses the travel characteristics of EV users in the study area based on the travel chain theory, using the latest data from a regional travel survey report. The experimental sample contains rich user travel information, which can reflect the common characteristics of social travel of general urban residents to a certain extent [27]. The travel state transfer matrix is built based on the daily number of trips, first travel moment, travel destination, and other major travel characteristics. It is then divided into four time periods to derive the user's travel state transfer probability [28]. The results are presented in Tables 4–7. They can be used to analyze the change in the transition probability of EV users within one day. In the OD matrix table, each functional area in the first column represents the "Origin" of the state transition process, and each functional area in the first row represents the "Destination" of the state transition process.

Table 4. OD probability matrix for electric vehicles in the early morning.

Proportion/(\%)	Residential	Workspace	Downtown	Public Service Area
Residential	0.1	0.5	0.2	0.2
Workspace	0.3	0.5	0.1	0.1
Downtown	0.3	0.3	0.3	0.1
Public service area	0.2	0.2	0.2	0.4

Table 5. OD probability matrix for electric vehicles in the lunchtime.

Proportion/(\%)	Residential	Workspace	Downtown	Public Service Area
Residential	0.1	0.2	0.6	0.1
Workspace	0.3	0.3	0.2	0.2
Downtown	0.5	0.2	0.2	0.1
Public service area	0.4	0.1	0.4	0.1

Table 6. OD probability matrix for electric vehicles in the evening.

Proportion/(\%)	Residential	Workspace	Downtown	Public Service Area
Residential	0.1	0.1	0.6	0.2
Workspace	0.6	0.1	0.2	0.1
Downtown	0.6	0.1	0.2	0.1
Public service area	0.7	0.1	0.1	0.1

Table 7. OD probability matrix for electric vehicles at night.

Proportion/ (%)	Residential	Workspace	Downtown	Public Service Area
Residential	0.1	0.1	0.7	0.1
Workspace	0.7	0.1	0.1	0.1
Downtown	0.6	0.1	0.2	0.1
Public service area	0.6	0.1	0.2	0.1

4. Electric Vehicle Charging Load Forecasting

The above statistics have obtained the characteristics of the regional distribution of travel needs of user groups. Based on the above statistics, the distribution of charging demand under different travel needs of electric vehicle users is predicted.

4.1. Improved Floyd Algorithm

Floyd algorithm calculates the distance matrix of a vertex-weighted graph using a series of n th order matrices. The algorithm determines the shortest path by evaluating the passable paths among all nodes in the network over several iterations. The traditional Floyd algorithm is shown in Equations (5) and (6).

$$l_{ij}^{(k)} = \min\{l_{ij}^{(k-1)}, l_{is}^{(k-1)} + l_{sj}^{(k-1)}\} \quad (5)$$

$$S_{ij}^{(k+1)} = \begin{cases} j, & l_{ij}^{(k)} = l_{ij}^{(k-1)} \\ s, & l_{ij}^{(k)} = l_{is}^{(k-1)} + l_{sj}^{(k-1)} \end{cases} \quad (6)$$

The Floyd algorithm traditionally requires the calculation of feasible path values between all nodes in the traffic network to determine the optimal path. However, this results in non-essential computations during multiple iterations, reducing computational efficiency and increasing storage space usage. To address this issue, this paper employs the Improved Floyd algorithm, which avoids redundant calculations [29].

Step 1 The weighted adjacency matrix based on the road network structure diagram is shown in Equation (7).

$$L^0 = (l_{ij}^{(0)})_{n \times n} (i, j = 1, 2, 3, \dots, n), k = 0 \quad (7)$$

Step 2 Find the value that does not need to be iterated at time $k + 1$. If $i = l_{ij}^{(k+1)}, l_{ij}^{(k+1)} = 0$; If ij is in a row with an infinite value and $l_{ij}^{(k)}$ is not infinite, then $l_{ij}^{(k+1)} = l_{ij}^{(k)}$; If $l_{is}^{(k)} \text{ or } l_{sj}^{(k)} \geq l_{ij}^{(k)}, l_{ij}^{(k+1)} = l_{ij}^{(k)}$.

Step 3 The values required for iteration are shown in Equation (8).

$$\begin{aligned} l_{ij}^{(k+1)} = \min\{l_{ij}^{(k)}, \min_{s < \min(i,j)} \{l_{\min(i,j),s}^{(k+1)} + l_{s,\max(i,j)}^{(k+1)}\}, \\ \min_{\min(i,j) < s < \max(i,j)} \{l_{\min(i,j),s}^{(k+1)} + l_{s,\max(i,j)}^{(k)}\}, \\ \min_{\max(i,j) < s} \{l_{\min(i,j),s}^{(k)} + l_{s,\max(i,j)}^{(k)}\} \} \end{aligned} \quad (8)$$

Step 4 If $L^{(k+1)} = L^{(k)}$, The current path matrix is the final result, and the iteration ends if this condition is met. Otherwise, return Step 2 to continue the iteration.

After comparison, it is evident that the Improved Floyd algorithm is less complex and more advantageous for calculating the shortest path of a complex road network. In this

paper, we obtained the shortest path for electric vehicles in the Anning District using the Improved Floyd algorithm.

4.2. Electric Vehicle Load Demand Forecasting Based on Monte Carlo Algorithm

The Monte Carlo algorithm is widely used in various fields, such as macroeconomics, theoretical physics, and finance. It is based on the theory of probabilistic statistics to solve the expected value of a method. In summary, the algorithm uses the law of large numbers to simulate the results of random sampling and approximate the computation results. The accuracy of the results increases with the number of samples [30].

The state of EV charging is stochastic at any given moment. The probability of the next state from the current charging state determines its shift. The future state is only dependent on the present state and its shifting probability, not on the previous state [31]. If we consider the SOC of the EV at a given moment as state S_i , and the SOC value of the EV at the next moment as state S_j , we can observe that state S_j is only related to S_i and its corresponding transfer probability p_{ij} at the current moment. The state transfer probability is shown in Equation (9).

$$p(S_i \rightarrow S_j) = p(S_i | S_j) = p_{ij} \quad (9)$$

The analysis focuses on the variation of SOC values and the prediction of charging loads for electric vehicles in a region throughout the day. All variables necessary for the prediction process are established.

(1) Possible user charging behavior is shown in Equation (10).

$$\begin{cases} a_k = 1, \text{Recharge} \\ a_k = 0, \text{neither Charging nor Driving} \\ a_k = -1, \text{Driving} \end{cases} \quad (10)$$

where a_k represents the charging behavior of the k th EV.

(2) The SOC value of electric vehicle users will change to a certain extent after charging. In this paper, it is assumed that the SOC value of electric vehicles changes in the range of $0.2 \leq SOC_k \leq 1$, and then the corresponding range of charging time can be introduced. As shown in Equations (11) and (12).

$$0.2 \leq \frac{CT_c}{Q_k} \leq 1 \quad (11)$$

$$\frac{0.2Q_k}{C} \leq T_c \leq \frac{Q_k}{C} \quad (12)$$

where C represents the charging power of the electric vehicle; T_c represents the charging duration; Q_k represents the battery capacity of the k th electric vehicle.

Taking different charging behaviors gives transfer probabilities for the corresponding behaviors as shown in Equation (13).

$$p_{ij} = \begin{cases} \int p\left(\frac{0.2Q_k}{C_k} \leq T_c \leq \frac{Q_k}{C_k}\right) f_T(T_c) dT_c, & a_k = 1 \\ 1, & a_k = 0 \\ F(l), & a_k = -1 \end{cases} \quad (13)$$

where p_{ij} is the state transition probability from state S_i to state S_j ; $p\left(\frac{0.2Q_k}{C_k} \leq T_c \leq \frac{Q_k}{C_k}\right)$ is the probability of electric vehicle users charging; $f_T(T_c)$ is the probability density function of the single charging duration T_c ; and $F(l)$ is the probability distribution of the user's single travel distance l , which is the integral of the probability density function of the single travel distance $f_l(l)$.

(3) SOC values for electric vehicles at the next moment

Given the SOC at the current moment and its charging behavior over a period of time from the current moment, the SOC of the EV at the next moment is derived.

When $a_k = 1$, the electric car is charged, as shown in Equation (14).

$$SOC_j = SOC_i + \frac{Ct_c}{Q_k} \quad (14)$$

When $a_k = 0$, the electric car is neither charged nor driven, as shown in Equation (15).

$$SOC_j = SOC_i \quad (15)$$

When $a_k = -1$, the electric vehicle is driven, as shown in Equation (16).

$$SOC_j = SOC_i - \frac{W_{100}l}{Q_k} \quad (16)$$

where l is the distance traveled by electric vehicle users in a single trip; W_{100} is the power consumption of electric vehicles per 100 km traveled.

Therefore, the SOC value of the electric vehicle at the next moment is obtained as shown in Equation (17).

$$SOC_j = \begin{cases} SOC_i + \frac{Ct_c}{Q_k}, & a_k = 1 \\ SOC_i, & a_k = 0 \\ SOC_i - \frac{W_{100}l}{Q_k}, & a_k = -1 \end{cases} \quad (17)$$

Through the above analysis, we can obtain the change in electric vehicle charging state transfer in one day, and we can obtain the electric vehicle charging load demand curve from the charging power accumulation of the charging process. By applying the Monte Carlo simulation method, the charging load demand of electric vehicles in a day is calculated, and the total charging load demand of electric vehicles in the region in one day can be obtained as shown in Equation (18).

$$SOC = \sum_{k=1}^N (SOC_j - SOC_i) \quad (18)$$

The Monte Carlo simulation steps are as follows, and its simulation flowchart is shown in Figure 8.

- Step 1 Determine the number of EVs in the study area, i.e., determine the number of Monte Carlo simulations; determine the number of different types of EVs and the corresponding parameters, such as battery capacity and corresponding charging power at charging piles;
- Step 2 According to the probabilistic model of charging start moment and start SOC established in the previous section, the charging start moment and the corresponding charging start SOC are randomly selected, and the EV charging duration is calculated;
- Step 3 This is used to simulate the recharging behavior of electric vehicle users after each trip in a day and to record the driving characteristics for each charge;
- Step 4 The charging load value of a single electric vehicle for a 24-h period is derived in 1-min simulation steps until all electric vehicles have been simulated, and the sum of the load demand for electric vehicles in each functional area is the forecast of the total demand for electric vehicle customer charging loads in the region in one day.

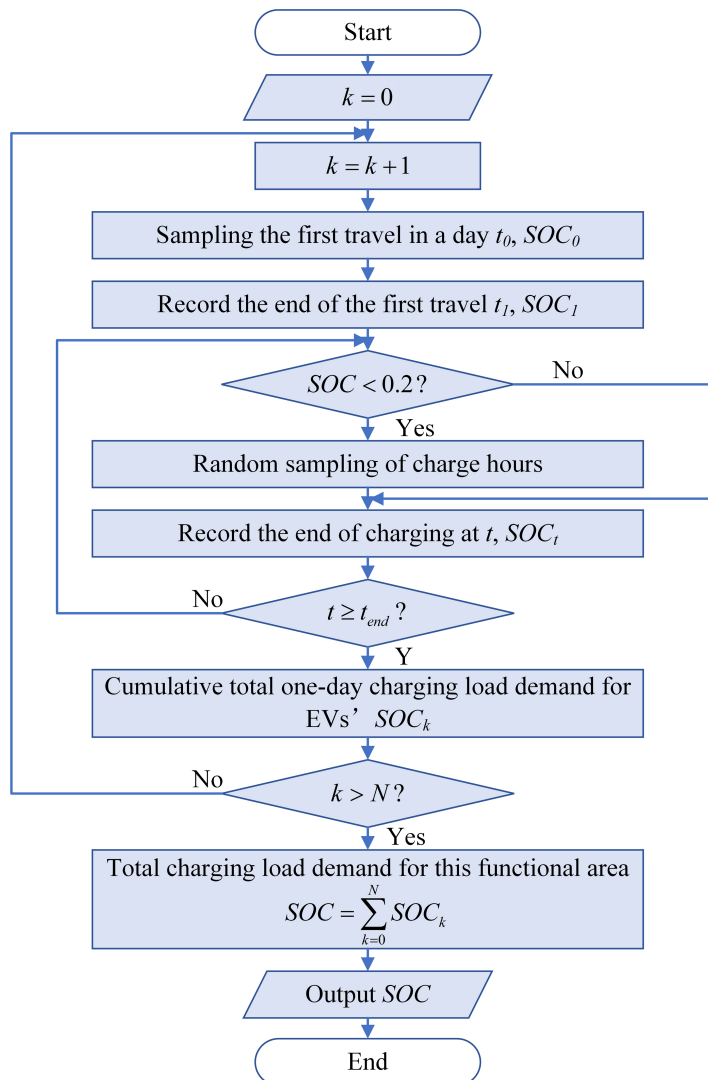


Figure 8. Monte Carlo load forecasting flowchart.

4.3. Electric Vehicle Load Demand Forecasting Based on Weighted Measurements Fused with UKF Algorithm Correction

4.3.1. Unscented Kalman Filter

The standard Kalman filter can only deal with the optimal estimation of linear systems, while the charging load of electric vehicles is a nonlinear dynamic system problem. If the Kalman filter is used directly to deal with the nonlinear system, the following problems will occur: first, the principle of superposition cannot be used, and the more iterations, the larger the error; second, the nonlinearity of the system results in the formulas no longer having simple recursive relationships with each other, so the standard Kalman filtering is not suitable for estimating the charging load of electric vehicles [32]. The extended Kalman filter is suitable for nonlinear systems, but this algorithm may introduce significant errors in the true posterior mean and covariance of the transformed Gaussian random variables, resulting in suboptimal or even divergent filter performance. As an extension of EKF, UKF can solve this problem through deterministic sampling methods and has the same computational complexity as EKF. Therefore, we chose the UKF with better performance and simpler calculation among the extended Kalman filter and the unscented Kalman filter [33].

The state equation of the discrete nonlinear multi-sensor system is shown in Equation (19).

$$\begin{cases} x(k+1) = f(x(k), k) + \omega(k) \\ z(k) = h(x(k), k) + v(k) \end{cases} \quad (19)$$

where x_k is the n-dimensional state vector; $f(\cdot)$ is the nonlinear system state function; $h(\cdot)$ is the system measurement function; $\omega(k)$ is the process noise of the system, which satisfies $\omega(k) \sim N\{0, Q(k)\}$; $z(k)$ is the multi-sensor measurement of the system; $v(k)$ is the measurement noise of the system, which satisfies $v(k) \sim N\{0, R(k)\}$.

UKF algorithm for nonlinear approximation via U-T transformation [34].

- (1) The sigma point sampling calculations are shown in Equation (20).

$$\chi_i(k|k) = \begin{cases} \bar{x}(k|k), i = 0 \\ \bar{x}(k|k) + \left[\sqrt{(n+k)P_{XX}(k|k)} \right]_i, i = 1, \dots, n \\ \bar{x}(k|k) - \left[\sqrt{(n+k)P_{XX}(k|k)} \right]_i, i = n+1, \dots, 2n \end{cases} \quad (20)$$

where χ represents the matrix of sigma vectors, $\sqrt{P_X}\sqrt{P_X}^T = P_{XX}$, P_X represents the variance of x , the i in $\left[\sqrt{(n+k)P_{XX}(k|k)} \right]_i$ represents the i -th column of the matrix root.

Sampling weights are shown in Equation (21).

$$\begin{aligned} W_i^m &= \begin{cases} \lambda/(n+k), i = 0 \\ 1/2(n+k), i \neq 0 \end{cases} \\ W_i^c &= \begin{cases} \lambda/(n+\lambda) + (1-\alpha^2 + \beta^2), i = 0 \\ 1/2(n+\lambda), i \neq 0 \end{cases} \end{aligned} \quad (21)$$

where $\lambda = \alpha^2(n+k) - n$ is a scaling factor, α is a scaling parameter that determines the distribution of sigma points in the surrounding area of \bar{x} and is adjusted to minimize the effect of higher order terms, and k is an adjustable parameter that can be adjusted to improve the degree of approximation [35].

- (2) Nonlinear propagation of sigma points.

The sigma points constructed above are non-linearly transformed according to formula $y = h(x)$ to produce the same number of transformed sample points Y_i as shown in Equation (22).

$$Y_i = h(\chi_i) \quad (22)$$

- (3) The mean and variance of y are calculated as shown in Equations (23) and (24) [36].

$$\bar{y} \approx \sum_{i=0}^{2n} W_i^m Y_i \quad (23)$$

$$P_y \approx \sum_{i=0}^{2n} W_i^c (Y_i - \bar{y})(Y_i - \bar{y})^T \quad (24)$$

Using the state estimates provided by UKF as a priori information to guide the Monte Carlo sampling process. First, a load demand prediction model considering EV charging behavior characteristics and grid load characteristics is established, which can describe the charging demand of different types of EVs in different charging periods [37]. The UKF algorithm is employed to approximate the state estimate of a nonlinear system using a series of sigma points. After obtaining the state estimates, sampling is performed using Monte Carlo methods to generate possible charging load scenarios that include different charging start times, charging powers, charging durations, etc. Multiple charging load

scenarios generated by Monte Carlo simulations are analyzed to identify potential peak load periods and charging demand patterns. Then, these scenarios are aggregated to form a forecast of the overall power grid load demand.

4.3.2. Weighted Measurement Fusion

Weighted measurement fusion(WMF) is a type of centralized data fusion that requires the measurement matrices of all sensors to be of the same dimension. In centralized data fusion, the measurement matrices of several sensors are sent to the fusion center, which makes a judgment based on the measurements of each observer and gives the optimal result. Weighted measurement fusion is where the measurements are processed in a least-squares sense and weighted at local nodes with a weighted average, where the weighted value is the inverse of the noise covariance of the individual measurements. The weighted fusion algorithm is shown in Figure 9. The sensor fusion technology employed primarily entails the integration of data from disparate sensors measuring the same quantity, with the objective of accurately determining the actual charging load. In Figure 9, the designation “Sensor 1, ..., Sensor N” refers to the sensors installed in a variety of electric vehicles, which are utilized to quantify the charging load demands of electric vehicle users from disparate geographical regions and categories of electric vehicles.

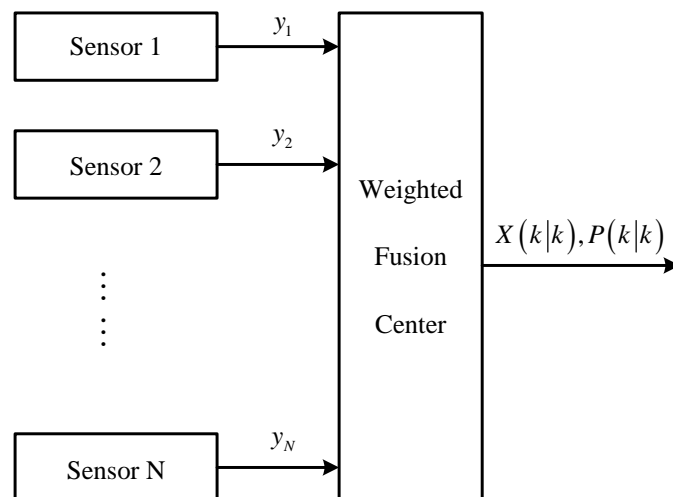


Figure 9. Weighted fusion mode.

The weighted fusion model is shown in Equations (25)–(27).

$$\hat{y} = \left[\sum_{i=1}^N (P^i)^{-1} \right]^{-1} \sum_{i=1}^N (P^i)^{-1} \hat{y}_i \quad (25)$$

$$H = \left[\sum_{i=1}^N (P^i)^{-1} \right]^{-1} \sum_{i=1}^N (P^i)^{-1} H_i \quad (26)$$

$$P = \left[\sum_{i=1}^N (P_i)^{-1} \right]^{-1} \quad (27)$$

where \hat{y} represents the weighted measurement value of each sensor; H represents the weighted measurement vector matrix; P represents the weighted measurement noise covariance.

4.3.3. WMF–UKF Corrected Load Forecasting

The EV charging measurement system and estimation system are nonlinear discrete systems. The electric vehicle load demand model is established based on the study of the weighted measurement UKF algorithm, as shown in Equation (28).

$$S_{k+1} = f(S_k, k) + \omega_k \quad (28)$$

where S_k is the EV charging load at moment k of the system; ω_k is the system noise.

For systematic observables, the relationship is as shown in Equation (29).

$$y_k^{(j)} = h(S(k), k) + v_k^{(j)} \quad (29)$$

where $y_k^{(j)}$ is the direct measurement of the EV charging load; $v_k^{(j)}$ is the noise generated during the measurement; and use the Monte Carlo prediction as the initial value for the system state variable $x(0)$. L represents the number of sensors in the system. Assuming $w(k)$ and $v^{(j)}(k)$ are zero mean and independent white noise, the variance matrices are Q and $R^{(j)}$. The relationship between the two satisfies Equation (30).

$$E\left(\begin{bmatrix} w(k) \\ v^{(j)}(k) \end{bmatrix} \begin{bmatrix} w^T(t) & v^{(j)T}(t) \end{bmatrix}\right) = \begin{pmatrix} Q & 0 \\ 0 & R^{(j)} \end{pmatrix} \delta_{kt} \quad (30)$$

where E is the mean number, T is the transpose number, $\delta_{kk} = 1$, $\delta_{kt} = 0(k \neq t)$, $\delta(\cdot)$ is the Dirac Delta function. $v^{(i)}(k)$ and $v^{(j)}(k)$ are independent of each other ($i \neq j$), as shown in Equation (31).

$$R^{(ji)} = E(\begin{bmatrix} v^{(j)}(t) & v^{(i)T}(k) \end{bmatrix}) = 0, j \neq i, \forall t, k. \quad (31)$$

The steps for filtering the EV charging load prediction system using the UKF algorithm are as follows.

- (1) Set initial value as shown in Equations (32) and (33).

$$\hat{S}_0 = E[S_0] \quad (32)$$

$$P_0 = E\left\{\left[S_0 - \hat{S}_0\right]\left[S_0 - \hat{S}_0\right]^T\right\} \quad (33)$$

- where \hat{S}_0 is the initial value of SOC; P_0 is the covariance of the state estimation error.
- (2) Forecast updates when $k > 1$, construct sigma points at moment $k - 1$ as shown in Equation (34) (set the number of sigma points to 3 [38]).

$$\begin{aligned} \vec{S}_{k-1}^{(0)} &= \hat{S}_{k-1} \\ \vec{S}_{k-1}^{(1)} &= \hat{S}_{k-1} + \sqrt{(1 + \lambda)P_{k-1}} \\ \vec{S}_{k-1}^{(2)} &= \hat{S}_{k-1} - \sqrt{(1 + \lambda)P_{k-1}} \end{aligned} \quad (34)$$

where $\lambda = 3\alpha^2 - 1$ is the scale parameter, and the tunable parameter α determines the degree of diffusion at the sigma points around \hat{S}_{k-1} . Calculate the predicted Sigma points and quasi-linearizing them according to the Taylor series expansion, as shown in Equation (35) [39].

$$\bar{S}_{k|k-1}^{(i)} = \vec{S}_{k-1}^{(i)} + \left(\frac{d\vec{S}}{dk}\right)_{k-1} \Delta k - \frac{\eta_{k-1}\Delta t}{C_n} I_{k-1}, i = 0, 1, 2 \quad (35)$$

where η is the EV charging efficiency and C_n is the EV battery capacity. Calculate the mean and variance of the predicted sigma points as shown in Equations (36) and (37).

$$\hat{S}_{k|k-1} = \sum_{i=0}^2 \omega_{(i)}^m \bar{S}_{k|k-1}^{(i)} \quad (36)$$

$$P_{k|k-1} = \sum_{i=0}^2 \omega_{(i)}^c \left[\bar{S}_{k|k-1}^{(i)} - \hat{S}_{k|k-1} \right] + Q_{k-1} \quad (37)$$

(3) Measurement updates

Let the measurement value of each sensor be y_k , the measurement matrix be $H_k^{(i)}$, and the measurement noise covariance be P_k .

The weighted measurements are shown in Equation (38).

$$y_k = \left[\sum_{i=1}^2 \left(P_k^{(i)} \right)^{-1} \right]^{-1} \sum_{i=1}^2 \left(P_k^{(i)} \right)^{-1} y_k^{(i)} \quad (38)$$

The weighted measurement vector is shown in Equation (39).

$$H_k = \left[\sum_{i=1}^2 \left(P_k^{(i)} \right)^{-1} \right]^{-1} \sum_{i=1}^2 \left(P_k^{(i)} \right)^{-1} H_k^{(i)} \quad (39)$$

The weighted measurement noise covariance is shown in Equation (40).

$$P_k = \left[\sum_{i=1}^2 \left(P_k^{(i)} \right)^{-1} \right]^{-1} \quad (40)$$

When a new measurement y_k is obtained, the system state values and variance are updated as shown in Equations (41)–(43).

$$\hat{S}_k = \hat{S}_{k|k-1} + K_k \left(y_k - \hat{y}_{k|k-1} \right) \quad (41)$$

$$P_k = P_{k|k-1} + K_k E_k K_k^T \quad (42)$$

$$K_k = G_k E_k^{-1} \quad (43)$$

where

$$\hat{y}_{k|k-1} = \sum_{i=0}^2 \omega_{(i)}^m \bar{y}_{k|k-1}^{(i)} \quad (44)$$

$$G_k = \sum_{i=0}^2 \omega_{(i)}^c \left(\bar{S}_{k-1}^{(i)} - \bar{S}_{k|k-1}^{(i)} \right) \left(\bar{y}_{k-1}^{(i)} - \bar{y}_{k|k-1}^{(i)} \right) \quad (45)$$

$$E_k = \sum_{i=0}^2 \omega_{(i)}^c \left(\bar{y}_{k|k-1}^{(i)} - \hat{y}_{k|k-1} \right) \left(\bar{y}_{k|k-1}^{(i)} - \hat{y}_{k|k-1} \right)^T + R_{k-1} \quad (46)$$

At any k moment, S_k is obtained as the initial value by Monte Carlo prediction [40]. After initialization, the prediction value \hat{S}_1 and the prediction error covariance P_1 of the EV SOC are obtained by the prediction and update equations; then calculate the process noise covariance Q_1 and the measurement noise covariance R_1 ; subsequently, the above-obtained values are used in the next prediction and update process. Repeating the process recursively yields the optimal prediction of the SOC of an electric vehicle in the time dimension.

5. Example Simulation

5.1. Data Pre-Processing

This paper analyses the electric vehicle historical travel data of a city and divides the travel destinations into four types: residential area, workspace, downtown, and public service area. The study area is located in northwest China with rugged terrain, and it can be seen from the road network structure that the distribution of major roads in the city is more concentrated, and the required data, such as highways, major roads, and secondary roads are retained according to the data attributes, and the processed road network data contains 17,036 lines of data. The main urban areas are analyzed as an example. The study has a generalized contribution to EV load demand forecasting in most cities in northwest China. And the average number of trips of electric private cars is 3.02 [41], and this paper assumes that the travel chain length of the private car is the longest of 3, and all of them are from the residential area to return to the residential area; the taxi shifts once every 24 h and takes a break of about 3 h between 2:00 and 5:00. Routine charging is performed during the break.

5.2. Analysis of Spatiotemporal Distribution of Charging Load

The spatial and temporal distribution of the EV charging load in the study area is obtained by dividing 24 h into 1440 time periods, each with a time step of 1 min. This is shown in Figure 10.

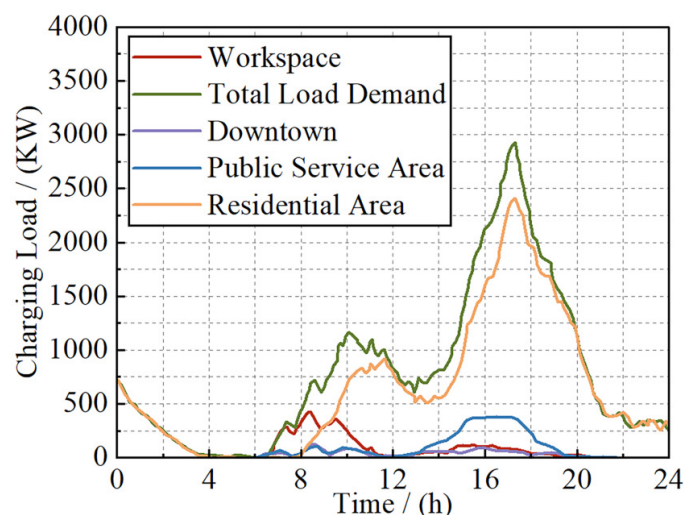


Figure 10. Load time distribution of private cars charging in different functional areas.

Figure 10 shows that the charging load demand in residential areas constitutes the largest proportion of the total load demand. This indicates that most private electric vehicles will choose to charge in residential areas; the charging load in workspace areas is concentrated in the period between 7:00 and 10:00, indicating that electric vehicle users are more willing to charge after arriving at the workspace and that the power after charging is likely to satisfy the next travel demand: Electric vehicle users have a stronger willingness to charge after arriving at the workspace, and the charged power is likely to satisfy the next traveling demand. Therefore, the demand for charging load after 12:00 is smaller. The charging load in commercial and public service areas is mainly concentrated between 15:00 and 19:00.

Figure 11 shows that electric taxis are concentrated in residential areas and workspaces in the period between 2:00 and 5:00 and between 15:00 and 23:00. The charging loads are higher in the early morning than in the afternoon. The total load demand is higher in residential areas and downtown and lower in workspaces and public service areas.

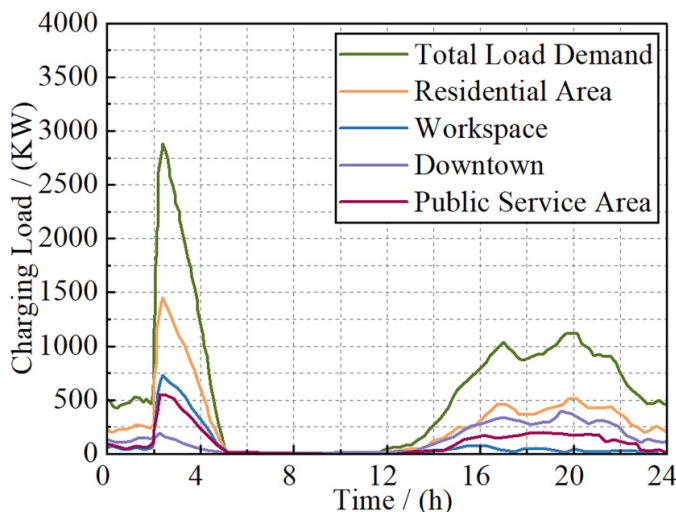


Figure 11. Load time distribution of taxi charging in different functional areas.

5.3. Comparative Analysis of Algorithm Accuracy

Furthermore, to assess the accuracy of the algorithm proposed in this paper, we simulated a total of 50,000 electric vehicles based on the electric vehicle ownership rate of 0.38 per household in the study area. The battery capacity of the electric vehicle is set to 20 kWh, with a charging power of 5 kW. Reference [12] analyzed the mobility characteristics and charging characteristics of various types of electric vehicles, combined Markov decision theory and Monte Carlo simulation methods to establish a spatial and temporal transfer model for various types of vehicles, and analyzed the charging load demand of electric vehicles in cities, taking into account the impact of real-time traffic conditions and temperature [12], which is similar to the method used in this paper. The method proposed in this paper and the reference method in reference [12] were used to perform the simulations and compare them with the actual load demand curve. The results are shown in Figure 12.

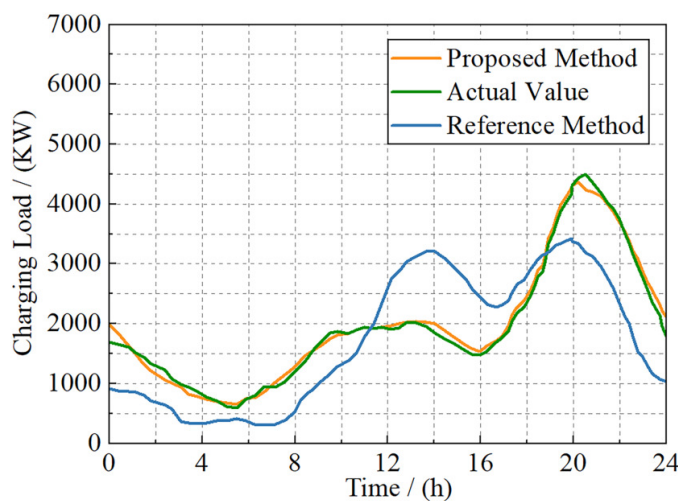


Figure 12. Comparison of load forecast values.

Figure 13 shows that there are two peak hours of load demand for EV charging each day. The load demand curve shows two peak values, one at 12:00 noon and the other at 8:00 p.m. The first peak value is lower than the second. Reference [12] also shows two peak values, one at 2:00 p.m. and the other at 8:00 p.m. The charging loads have peak values that are relatively close to each other. The proposed method's load demand curve also has two peak values, one at 12:00 noon and the other at 8:00 p.m. The recorded peak

demand values occur at 12:00 noon and 8:00 p.m., which is consistent with the actual load demand values. Notably, the first peak value is lower than the second peak value. This paper comprehensively considers the charging load demand of four functional areas. The downtown and public service areas have concentrated charging peaks during daytime hours, with longer overall duration and smaller peaks. On the other hand, the workspace and residential areas have obvious peak hours with shorter durations and larger load peaks. After conducting an overlay analysis, it was found that the trend of load demand peaks during daytime hours is low and slow, while the trend of evening peak values is high and steep.

This paper calculates the error and root mean square error of the predicted values for both the method proposed in this paper and the method presented in reference [12]. Figures 13–15 show that the method proposed in this paper has a small deviation from the actual value, with a maximum error of about 300 kW. In contrast, the load prediction value of the reference method has a large deviation from the actual value, with a maximum error of up to 1300 kW.

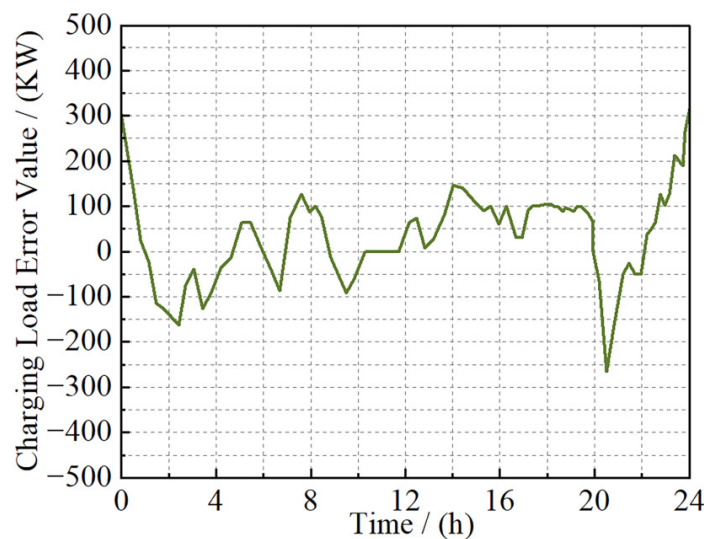


Figure 13. Predictive value errors of WMF-UKF.

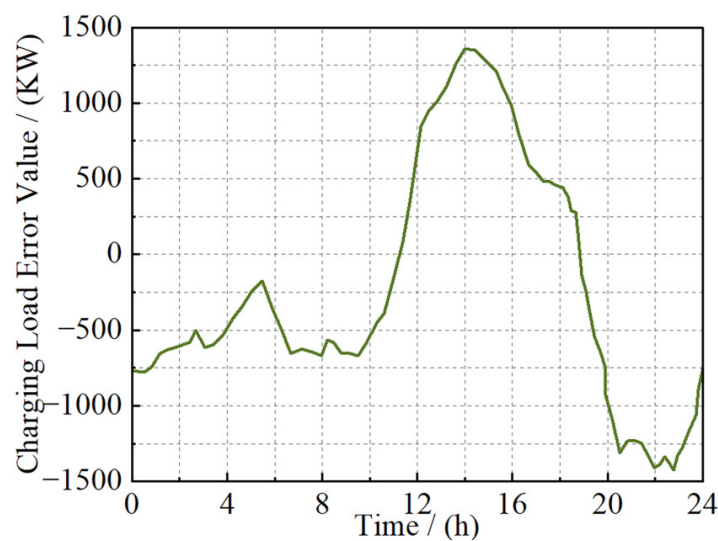


Figure 14. Predictive value errors of MDP random path simulation.

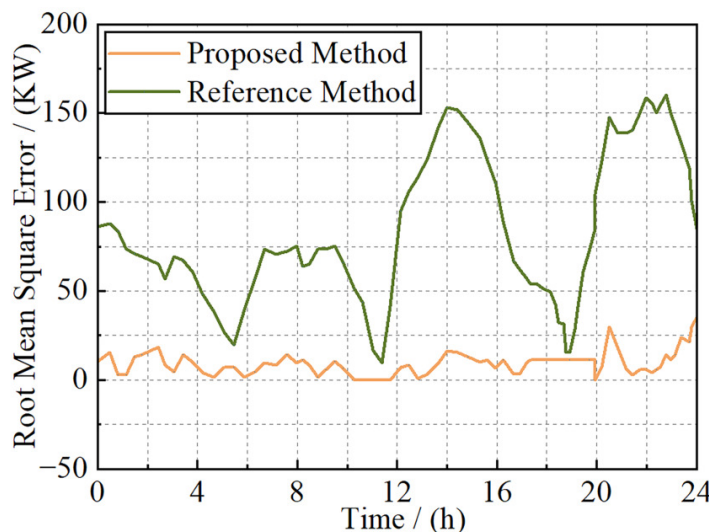


Figure 15. Root means square error of predictions for both methods.

Figure 15 shows that the mean square deviation of the load forecast values in reference [12] is larger than that of the algorithm proposed in this paper. Compared to reference [12], the proposed method in this paper improves the first peak prediction accuracy by 53.53% and the second peak prediction accuracy by 23.23%. Therefore, the proposed method in this paper has a higher accuracy for regional EV load demand forecasting and a more accurate prediction of the peak load and its occurrence time.

To demonstrate the advantages of the algorithm proposed in this paper in terms of statistical significance, we have calculated the mean square error (MSE), the mean absolute error (MAE), and the coefficient of determination (R^2) between the predicted and the actual values of the algorithm as well as comparing it with the other methods in the existing references. The results of the comparison of the error metrics are shown in Table 8.

Table 8. Comparison of error indicators.

Scheme	MSE	MAE	R^2
WMF–UKF	1170.18 kW	46.0307 kW	0.89
MDP random path simulation	7439.55 kW	319.895 kW	0.57

5.4. Industrial Field Verification

Applying this study to EV private car users charging load demand forecasting in Anning District, Lanzhou City. The road network structure and distribution of electric vehicles in the study area are shown in Figure 16. According to the road attributes to exclude sidewalks, parkways, and other irrelevant sections, the ArcGIS processed road network data contains 1350-line data and 800-point data. Set the charging behavior when the EV load state is less than 0.2 SOC.

Applying the algorithm proposed in this paper to compare the actual demand value and the predicted value of electric vehicle charging load in one day in Anning District. The results are shown in Figure 17.

The comparison illustrates the superiority of using the algorithm proposed in this paper to predict the load demand of electric vehicles in the study area with higher accuracy and more closely match the actual load demand values.



Figure 16. Electric vehicle distribution in Anning district.

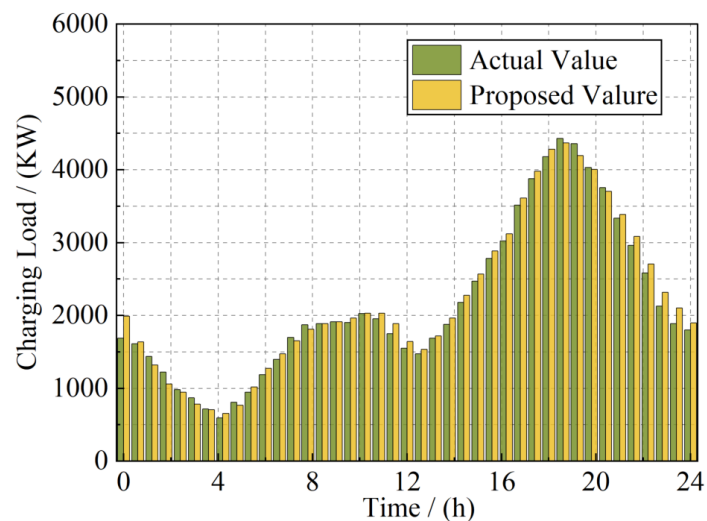


Figure 17. Comparison of forecast and actual electric vehicle load demand in Anning District.

6. Conclusions

In this paper, a predictive control method is proposed for the electric vehicle charging load demand model by applying a weighted measurement fusion unscented Kalman filter algorithm, with the study area divided into multiple functional zones. Through verification, the following conclusions are drawn.

- (1) ArcGIS-based modeling of urban functional areas and road networks is simpler and more flexible than the traditional methods of road network modeling. This is conducive to the analysis of the spatial and temporal distribution of urban electric vehicle load demand.
- (2) The demand for charging urban EVs concentrates in residential and downtown areas. In residential areas, the demand for charging is the highest, while it is the opposite in workspace and public service areas.
- (3) Urban electric vehicles show two peaks in charging load demand during the day. The first peak appears at around 12:00, and the second one appears at around 8:00 p.m., with the midday peak below the evening peak.
- (4) The algorithm intended for the WMF–UKF achieves a higher accuracy. Compared to the existing methods as a reference, the accuracy of predicting the first peak of the charging load demand is improved by 53.53%, and that of predicting the second peak

is improved by 23.23%. This method enhances the accuracy in forecasting the spatial and temporal distribution of EV load demand.

To conclude, the method proposed in this paper can enhance the accuracy of EV load demand prediction. Analyzing the spatial and temporal distribution of load demand in different functional areas of the city provides a practical reference for future research on site selection and capacity planning for EV charging stations, as well as for the research on connecting EVs to the power distribution network.

Author Contributions: Conceptualization, M.T.; Data curation, X.G.; Formal analysis, X.G., J.L. and B.A.; Funding acquisition, M.T.; Investigation, X.G., J.Q., J.L. and B.A.; Methodology, M.T., X.G. and J.Q.; Project administration, M.T.; Resources, M.T. and J.L.; Software, X.G.; Supervision, M.T. and J.Q.; Validation, J.Q., J.L. and B.A.; Visualization, X.G. and J.Q.; Writing—original draft, M.T. and X.G.; Writing—review and editing, M.T. and J.Q. All authors have read and agreed to the published version of the manuscript.

Funding: The first author is supported by the National Natural Science Foundation of China [grant numbers 62363022, 61663021, 71763025, and 61861025]; Natural Science Foundation of Gansu Province [grant number 23JRRA886]; Gansu Provincial Department of Education: Industrial Support Plan Project [grant number 2023CYZC-35].

Data Availability Statement: The raw data supporting the conclusions of this article will be made available by the authors on request.

Conflicts of Interest: The authors declare no conflicts of interest.

Abbreviations

The following abbreviations are used in this manuscript:

OD	Origin destination
EV	Electric vehicle
WMF	Weighted measurement fusion
SOC	State of charge
Mc	Monte Carlo
UKF	Unscented Kalman filter
EKF	Extended Kalman filter
Variables	
p	Transfer probability
L	The number of sensors in a discrete nonlinear multi-sensor system
C	Charging power
Q/R	Variance
P	Weighted covariance of measurement noise from multiple sensors
P_y	Covariance of y
y_k	measurement values of the SOC of EVs at time k
K_k	UKF gain
E_k	Filter covariance at time k
G_k	Filter cross-covariance at time k

References

1. Hua, Y.; Wang, Y.; Han, D.; Bu, F.; Wang, H.; Jia, Y.B. Medium and long-term charging load forecasting of electric vehicles in residential areas considering orderly charging. *J. Power Syst. Autom.* **2022**, *34*, 142–150.
2. Luo, Z.; Hu, Z.; Song, Y.; Yang, X.; Zhan, K.; Wu, J.Y. Electric vehicle charging load calculation method. *Power Syst. Autom.* **2011**, *35*, 30–42.
3. Yi, F.; Li, F. An exploration of a probabilistic model for electric vehicles residential demand profile modeling. In Proceedings of the 2012 IEEE Power and Energy Society General Meeting, San Diego, CA, USA, 22 July 2012; pp. 1–6.
4. Chen, L.; Yang, F.; Xing, Q.; Wu, S.; Wang, R.; Chen, J. Spatial-temporal distribution prediction of charging load for electric vehicles based on dynamic traffic information. In Proceedings of the 2020 IEEE 4th Conference on Energy Internet and Energy System Integration (EI2), Wuhan, China, 30 October 2020; pp. 1269–1274.
5. Jawad, S.; Liu, J. Electrical Vehicle Charging Load Mobility Analysis Based on a Spatial-Temporal Method in Urban Electrified-Transportation Networks. *Energies* **2023**, *13*, 5178. [[CrossRef](#)]

6. Ding, L.; Ke, S.; Zhang, F.; Lin, X.; Wu, M.; Zhang, J.; Yang, J. Electric vehicle charging load forecasting considering travel demand and guidance strategies. *Electr. Power Constr.* **2024**, *48*, 1000–1029.
7. Zhang, M.; Xu, L.; Yang, X. Electric vehicle charging demand forecasting based on city grid attribute classification. *Electr. Meas. Instrum.* **2022**, *48*, 592–597.
8. Aduama, P.; Zhang, Z.; Al-Sumaiti, A. Multi-feature data fusion-based load forecasting of electric vehicle charging stations using a deep learning model. *Energies* **2023**, *16*, 1309. [[CrossRef](#)]
9. Xu, L.; Chen, Y.; Wang, Y.; Li, N.; Zong, Q.; Chen, K. Research on Electric Vehicle Ownership and Load Forecasting Methods. In Proceedings of the 2020 5th International Conference on Mechanical, Control and Computer Engineering (ICMCCE), Harbin, China, 25–27 December 2020; pp. 184–188.
10. Aduama, P.; Zhang, Z.; Al-Sumaiti, A. Short-term charging load prediction for electric vehicles with federated learning accounting for user charging behavior and privacy protection. *High Volt.* **2023**, *1*–8.
11. Chen, Y.; Jiang, Y.; Xu, G.; Cui, J.; Qing, D.; Zhu, X. Load forecasting of electric vehicles based on Monte Carlo method. In Proceedings of the 2020 5th International Conference on Mechanical, Control and Computer Engineering (ICMCCE), Harbin, China, 25–27 December 2020; pp. 1203–1206.
12. Zhang, Q.; Wang, Z.; Tan, W.; Liu, H.; Li, C. Spatial-temporal distribution prediction of electric vehicle charging load based on MDP random path simulation. *Power Syst. Autom.* **2018**, *42*, 59–66.
13. Zhou, B.; Li, E. Multi-Regional integrated energy economic dispatch considering renewable energy uncertainty and electric vehicle charging demand based on dynamic robust optimization. *Energies* **2024**, *11*, 2453. [[CrossRef](#)]
14. Li, H.; Song, Y.; Li, S.; Zhu, Y.; Kang, Y.; Dong, H. Electric vehicle charging load forecasting method based on ArcGIS road network structure and traffic congestion analysis. *Grid Technol.* **2024**, *42*, 1–14.
15. Zhang, N.; Tao, H.; Liu, Y.; Cui, J.; Yang, J.; Gang, W. Short-term load forecasting algorithm based on LSTM-DBN considering the flexibility of electric vehicle. *Iop Conf. Ser. Earth Environ. Sci.* **2020**, *546*, 1715–1755.
16. Zhou, D.; Zhong, H.; Yu, Z.; Yu, H.; Da, J.; Yi, B.; Dong, L. Using bayesian deep learning for electric vehicle charging station load forecasting. *Energies* **2022**, *17*, 6195. [[CrossRef](#)]
17. Liu, X.; Teng, H.; Gong, Y.; Teng, D. Short-term load forecasting based on improved Kalman filtering algorithm. *Electr. Meas. Instrum.* **2019**, *56*, 42–46.
18. Li, Y.; Sun, S.; Hao, G. Nonlinear weighted observation fusion of traceless Kalman filters based on Gauss-Hermite approximation. *J. Autom.* **2019**, *45*, 593–603.
19. Yao, L.; Huang, S.; Gao, Z. Electric vehicle charging load forecasting based on deep learning and spatio-temporal analysis. *Appl. Energy* **2023**, *319*, 119731.
20. Wang, J.; Liu, P.; Hao, H. Modeling and forecasting the charging load of electric vehicles: A comprehensive review. *Renew. Sustain. Energy Rev.* **2023**, *164*, 112573.
21. Chen, Q.; Xue, L.; Sun, H. Probabilistic forecasting of electric vehicle charging load based on conditional variational autoencoder. *Energy* **2023**, *256*, 124685.
22. Zhang, X.; Li, Y.; Gao, W. Charging load prediction for electric vehicles using machine learning and spatial-temporal analysis. *Leee Trans. Smart Grid* **2024**, *15*, 1234–1246.
23. Wu, C.; Gao, F.; Xu, Z. Probabilistic forecasting of electric vehicle charging load based on conditional variational autoencoder. *Leee Access* **2024**, *12*, 45678–45690.
24. Ye, P.; Chen, X. Method of urban road classification based on road skeleton. *J. Tongji Univ. Nat. Sci. Ed.* **2011**, *39*, 853–856+878.
25. Elahe, M.; Kabir, M.; Mahmud, S.; Azim, R. Factors impacting short-term load forecasting of charging station to electric vehicle. *Electronics* **2022**, *12*, 55. [[CrossRef](#)]
26. Wang, Y. *Prediction of Electric Vehicle Charging Demand Based on Urban Travel Characteristics*; Northern Polytechnic University: Xi'an, China, 2022.
27. Luo, Q. *Application of Electric Vehicle Charging Station Location and Capacity Based on Improved Sparrow Search Algorithm in Planning Area*; Northeast Petroleum University: Daqing, China, 2022.
28. Sha, X. *Research on Coordinated Charging Strategy for Electric Vehicles Considering Network Load Interaction*; Hangzhou Dianzi University: Hangzhou, China, 2023.
29. Ma, J. *Research on Charging Station Layout Optimization and Orderly Charging and Discharging Strategy Based on Spatial and Temporal Distribution Prediction of Electric Vehicle Charging Load*; Xi'an University of Technology: Xi'an, China, 2023.
30. Ma, R. *Research on the Optimal Scheduling of Distribution Network Based on the Spatial and Temporal Distribution Characteristics of Electric Vehicle Charging Demand*; Xi'an University of Technology: Xi'an, China, 2023.
31. Yang, M.; Zhou, S.; Gu, J. Data-driven OD prediction of urban residents. *Nat. Sci. Ed.* **2022**, *19*, 73–80.
32. Xu, D.; Cai, M.; Chen, Y. Shortest path planning of urban traffic network based on improved Floyd algorithm. *Electronics* **2017**, *30*, 17–20.
33. Zhao, H.; Tian, B. Robust Power System Forecasting-Aided State Estimation With Generalized Maximum Mixture Correntropy Unscented Kalman Filter. *IEEE Trans. Instrum. Meas.* **2022**, *71*, 1–10. [[CrossRef](#)]
34. Li, X.; Xiao, H.; Li, J. Research on electric vehicle charging load forecasting using Kalman filter modified Monte Carlo algorithm. *Sichuan Electr. Power Technol.* **2019**, *42*, 37–40+50.

35. He, P.; Ji, P.; Chen, J. Application of Unscented Kalman Filter Algorithm in Short term Load Forecasting. *Electr. Switch.* **2015**, *53*, 81–85.
36. Hao, G.; Ye, X.; Chen, T. Weighted measurement fusion nonlinear unscented Kalman filter algorithm. *Control Theory Appl.* **2011**, *42*, 753–758.
37. Sun, F.; Hu, X.; Zou, Y.; Li, S. Adaptive unscented Kalman filtering for state of charge estimation of a lithium-ion battery for electric vehicles. *Energy* **2011**, *36*, 3531–3540. [[CrossRef](#)]
38. Lv, L.; Xu, W.; Xiang, Y.; Zhang, Y.; Xiong, J. Research on Optimization Configuration of Multi area Charging Stations Based on Markov Chain Charging Load Prediction. *Eng. Sci. Technol.* **2017**, *49*, 170–178.
39. Wang, W.; Wang, X.; Xiang, C.; Wei, C.; Zhao, Y. Unscented Kalman filter-Based battery SOC estimation and peak power prediction method for power distribution of hybrid electric vehicles. *IEEE Access* **2018**, *6*, 35957–35965. [[CrossRef](#)]
40. Zhao, S.; Zhou, J.; Li, Z.; Zhang, S. Electric vehicle charging demand analysis method based on trip chain theory. *Electr. Power Autom. Equip.* **2017**, *37*, 105–112.
41. Wang, Y.; He, G.; Liu, Y. Multi-sensor tracking fusion algorithm based on Kalman filter. *Ship Power Technol.* **2013**, *33*, 4–7.

Disclaimer/Publisher’s Note: The statements, opinions and data contained in all publications are solely those of the individual author(s) and contributor(s) and not of MDPI and/or the editor(s). MDPI and/or the editor(s) disclaim responsibility for any injury to people or property resulting from any ideas, methods, instructions or products referred to in the content.